First Exploration on a Poly(vinyl chloride) Ultrafiltration Membrane Prepared by Using the Sustainable Green Solvent PolarClean

First Exploration on Poly (vinyl chloride) Ultrafiltration Membrane Prepared by Using the Sustainable Green Solvent PolarClean

Wancen Xie, [†] *Alberto Tiraferri,* [‡] *Baicang Liu,* [†,*] *Peng Tang,* [†] *Fang Wang,* [§] *Sheng Chen,* [//] *Alberto Figoli,* [⊥] *Liang-Yin Chu* [§]

[†] Institute of New Energy and Low-Carbon Technology, College of Architecture and Environment, Sichuan University, No. 2, Section 2, Chuanda Rd., Chengdu, Sichuan 610207, People's Republic of China

[‡] Department of Environment, Land and Infrastructure Engineering, Politecnico di Torino, Corso Duca degli Abruzzi 24, 10129 Turin, Italy

[§] School of Chemical Engineering, Sichuan University, No. 24, South Section 1, Yihuan Rd., Chengdu, Sichuan 610065, People's Republic of China

[*] Corresponding author.

Tel.: +86-28-85995998; fax: +86-28-62138325; e-mail: bcliu@scu.edu.cn; baicangliu@gmail.com (B. Liu).

[∥] College of Biomass Science and Engineering, Sichuan University, No. 24, South Section 1, Yihuan Rd., Chengdu, Sichuan 610065, People's Republic of China

[⊥] Institute on Membrane Technology ITM-CNR, Via P. Bucci 17/C, 1-87030 Rende, Cosenza, Italy

KEYWORDS: Poly (vinyl chloride) PVC; Green solvent; PolarClean; Ultrahigh permeability; Ultrafiltration

ABSTRACT: Large-scale membrane fabrication currently relies on the use of traditional solvents, such as N, N-dimethylacetamide, 1-methyl-2-pyrrolidinone, and dimethylformamide. These solvents are toxic, slowly biodegradable and combustible, posing risks to human health and the environment, and requiring careful safety procedures. Replacing traditional solvents with green solvents while maintaining or improving the membrane performance is a challenging task at the forefront of research and development in the field of membrane technology. We employed a novel green solvent, methyl-5-(dimethylamino)-2-methyl-5-oxopentanoate (Rhodiasolv® PolarClean), to prepare high-performance poly (vinyl chloride) ultrafiltration membranes. This green solvent was used to completely replace toxic solvents during membrane synthesis, for the first time. The effects of polymer concentration, addition of amphiphilic copolymer poly (vinyl chloride)-graft-poly (ethylene glycol) methyl ether methacrylate concentration, and use of a non-woven polyethylene terephthalate fabric as support layer were investigated systematically. The membrane fabricated with 8% PVC, 5% PVC-g-PEGMA, and non-woven PET fabrics as support layer showed the best overall performance, presenting small and narrowly distributed membrane pores, high surface porosity, smooth surface, ultrahigh ~~membrane~~ pure water permeability coefficients of >5000 L $m^{-2}h^{-1}bar^{-1}$ ~~when pure water was used~~, high sodium alginate rejection of nearly 98%, and flux recovery ratio of 57 %. This study demonstrates the feasibility of using green solvent to increase the sustainability and effectiveness of membrane processes.

INTRODUCTION

Membrane separation technologies have wide-range applications in the food, biotechnology, and dairy industry, as well as in water treatment, thanks to their simple operating equipment, high efficiency and low energy consumption,[1] often representing sustainable alternatives to traditional technologies. [2] Among the numerous membrane materials, poly (vinyl chloride) (PVC) is one of the most common owing to its low-cost, acid-alkali-microbial resistance, and good mechanical strength. [3-6] Unfortunately, the application of PVC membranes is limited by their inherent low flux and because they are prone to fouling. [4, 7] Important efforts are currently spent to increase the performance and antifouling properties of these membranes. [8]

The most widely adopted modification method to improve PVC-based membranes is blending, in which hydrophilic or amphiphilic additives are added to the dope solution during casting. The blending method is simple and reliable. [9] Our previous study investigated the amphiphilic copolymer poly (vinyl chloride)-graft-poly (ethylene glycol) methyl ether methacrylate (PVC-g-PEGMA) as a blending additive for PVC, allowing the enhancement of the membrane pure water flux and antifouling properties. [10] The solvent used during synthesis was traditional N, N-dimethylacetamide (DMAc), a well-established favorable solvent for PVC. [11]

The solvents used in membrane casting play an important role in dissolving polymers and additives, and are large determinants of the final membrane characteristics. [9, 12] Unfortunately, the solvents currently employed by membrane manufacturers are harmful and toxic; their vast use poses great risks to the environment, health and safety (EHS), and is not in agreement with the twelve principles of green chemistry. [13-15] Some greener and more sustainable solvents have been proposed to substitute traditional solvents in recent years. [16] Triethyl phosphate (TEP) is a safer solvent [14, 15] and only harmful when being swallowed or when in contact with the eyes. [17]

However, this compound cannot be defined as a "green" solvent. [2] TEP has good affinity with poly (vinylidene fluoride) (PVDF) and has thus been used to fabricate membranes from this material. [13, 17-20]. Dimethyl sulfoxide (DMSO) is a model safer solvent because it is non-toxic, clean, and recyclable, [2, 21] and it can dissolve many polymers [21]. There has been work on PVDF [22, 23], polyacrylonitrile (PAN) [24], polyethersulfone (PES) [25-27], and polyimide P84® [28] membranes fabricated using DMSO as solvent. Other benign solvents have also been reported, for example, diluent acetyl tributyl citrate (ATBC) [29-31] or triethylene glycol diacetate (TEGDA). [32] Ionic liquids (ILs) are another class of green solvents, which have negligible volatility, and can be recycled and reused repeatedly. [33] Xing et al. [34, 35] successfully used a 1-ethyl-3-methylimidazolium acetate ([EMIM]OAc) to fabricate ultrafiltration membranes. Facal and co-workers [36] also successfully employed ionic liquids to obtain cellulose-based hollow fiber membranes.

Methyl-5-(dimethylamino)-2-methyl-5-oxopentanoate (Rhodiasolv® PolarClean, in the following abbreviated as PolarClean) is a new highly promising member of the green solvent family. This compound is derived from 2-methylglutaronitrile (MGN), a by-product of Nylon 66 manufacturing otherwise needing disposal. [37-39] PolarClean is entirely biodegradable (97% in 18 days) and it is associated with low carbon footprint based on the Rhodia raw material database. Furthermore, it has no or little environment or health hazards. Finally, it is nonflammable and has very low vapor pressure. [40] LCA analyses have confirmed that PolarClean has much lower environmental effects compared to other common solvents used for membrane preparation. [37, 41-45] In summary, the use of PolarClean may reduce the total CO_2 emission and the environmental impacts of the membrane manufacturing phase. There are some reports on PVDF, [40, 46, 47] PES [48, 49] and Matrimid® 5218 [50] membranes cast using the solvent PolarClean. For example, Wang et al.

[49] fabricated polysulfone (PSF) and PES ultrafiltration membranes, as well as cellulose acetate (CA) nanofiltration membrane starting from a PolarClean dope solution, thus demonstrating the general feasibility of this solvent in membrane preparation. As of now, no PVC membrane have been prepared using PolarClean and this represents a significant deficiency in this field, due to the importance and applications of PVC membranes.

The great challenge of using green solvents is establishing the correct synthesis route to achieve comparable performance with that shown by membranes fabricated with traditional solvents. Our previous study using mixtures of DMSO, NMP, and DMAc to fabricate PVC/PVC-g-PEGMA membranes has proven that correct recipes and synthesis protocols can provide the desired performance. [51] In fact, the membrane had improved pure water flux, sodium alginate (SA) rejection, and antifouling properties. In this study, we employ the green solvent PolarClean to completely replace all the toxic solvents for the fabrication of PVC-based membranes. This research also explores the effect of several parameters, including the relative concentrations of PVC and PVC-g-PEGMA in the dope solution and the use of a non-woven polyethylene terephthalate (PET) fabric. The main objectives are thus to identify the most suitable synthesis protocol and to demonstrate the feasibility of using single solvent PolarClean to obtain high-performance PVC-based ultrafiltration membranes.

MATERIALS AND METHODS

Chemicals and Materials. PolarClean was kindly provided by Solvay Specialty Polymers (Shanghai, China). Poly(vinyl chloride) (PVC, high molecular weight), poly(ethylene glycol)methylethermethacrylate (PEGMA, Mn = 500 g/mol), 1,1,4,7,10,10-hexamethyltriethylenetetramine (HMTETA, 97%), copper(I) chloride (CuCl, ≥ 99.995%), 1-

methyl-2-pyrrolidinone (NMP, anhydrous, 99.5%), N,N-dimethylacetamide (DMAc, 99%), sodium alginate (SA), and sodium chloride (NaCl, reagent grade, 99%) were obtained from MilliporeSigma (St. Louis, MO, USA). Methanol (99.9 %) and dimethyl sulphoxide-d_6 (DMSO-d_6, 99.9%) were obtained from Kelong Chemical (Chengdu, China).

Synthesis of the Graft Copolymer PVC-g-PEGMA. The synthesis procedures were similar to our previous study, [10, 51] and the details are listed in Text S1 (Supporting Information, SI). The successful synthesis was proven by ^{1}H nuclear magnetic resonance (NMR, AVANCE AV II-600, Bruker, Switzerland). Before NMR analysis, the sample (15 mg) was dissolved in DMSO-d_6 (0.5 mL) and heated for 24 h to ensure complete dissolution. Subsequently, ^{1}H NMR spectra were recorded at 600 MHz. The ^{1}H NMR results and analysis are reported in Figure S1 and Text S5 (SI).

Fabrication of PVC UF Membranes. The compositions of the membrane casting solutions are shown in Table 1. The membranes were prepared via nonsolvent induced phase separation (NIPS), and the procedures are presented in detail in Text S2 (SI).

Table 1. Composition of PVC Membrane Casting Solutions.

Membrane	PVC (g)	PVC-g-PEGMA (g)	PolarClean (g)	DMAc (g)	Additive/PVC (w/w %)	Thickness of the support layer (μm)
M1-6P[a]	6	0	94	-	0	-
M2-8P	8	0	92	-	0	-
M3-10P	10	0	90	-	0	-
M4-8DMAc	8	0	-	92	0	-
M5-5P-g-P[b]	8	0.4	91.6	-	5	-
M6-10P-g-P	8	0.8	91.2	-	10	-
M7-15P-g-P	8	1.2	90.8	-	15	-
[c] M8-5P-g-P^{SL}	8	0.4	91.6	-	5	29 ± 2

Note: [a] P means pure PVC membranes. [b] P-g-P means PVC blended PVC-g-PEGMA membranes. [c] SL means PVC membranes with support layer.

Ternary phase diagram determination. The cloud points for the casting solutions of M1-M7 were measured by titration. After the complete dissolution of all components in PolarClean or DMAc, DI water was added to the solutions at 60 ℃ while stirring at 500 rpm. DI water was added slowly and up until the solution did no longer become homogeneous within 24 h. [52, 53]

Characterizations and Analyses. The membrane surface and cross-sectional morphologies were observed by scanning electron microscopy (SEM) (SU200, Hitachi, Japan). The membrane samples were fixed onto the conductor tape and sputter-coated with a ~ 2 nm gold layer. Coated samples were observed with a 5 kV acceleration voltage under different magnifications. The cross-sectional samples were pretreated with liquid nitrogen for roughly 15 min before sputtering. The membrane surface roughness was obtained by atomic force microscopy (AFM, MultiMode 8,

Bruker, Germany) with the scan rate of 1.00 Hz and the scan size of 5 μm × 5 μm. Every membrane sample was analyzed in at least four different locations and the average value was calculated.

The elemental composition of near-surface depths < 5 nm was detected by X-ray photoelectron spectroscopy (XPS) (Axis Supra, Kratos Analytical Ltd., UK). The XPS spectra were obtained in the range 0-1100 eV of electron binding energy with a resolution of 1 eV. High-resolution spectra of the C 1s region were also obtained, and peak fitting was conducted under linear background. Attenuated total reflectance Fourier transform infrared (ATR-FTIR) spectra were obtained with a FTIR spectrometer (IRTracer-100, Shimadzu Co., Japan). The wavenumber range was 4000-650 cm^{-1}, and 64 scans were performed with a 2 cm^{-1} resolution. ATR-FTIR can detect deeper than 300 nm when wavenumbers are below 2000 cm^{-1}. [54] The dynamic water contact angles at the membrane surface were measured with a KRÜSS DSA 25S instrument (KRÜSS GmbH, Germany). A 2 μL droplet of DI water was placed onto the membrane surface, then the contact angle was recorded every 10 seconds for the overall duration of 170 s. For each membrane, at least nine replicate experiments were conducted to ensure reliable results.

Estimation of Membrane Total Porosity. The membrane total porosity was estimated using a water soaking method at room temperature, [6, 55] and the details of this method are listed in Text S3 (SI). The total porosity was calculated by the following equation (1).

$$\varepsilon\ (\%) = \frac{W_1 - W_2}{\rho_w A \delta} \times 100 \qquad (1)$$

where ρ_w (g/cm^3) is the density of pure water (0.998 g/cm^3) and A (cm^2) is the area of the wet membrane (4 cm^2). At least four replicate experiments were performed for ~~every~~ each membrane.

Ultrafiltration Performance Tests. The steps for the characterization of the membrane transport properties were the same as discussed in our previous study, [10, 51] and are presented in

Text S4 (SI). The pure water permeability coefficient of the membrane, which was obtained from ~~pure water~~ flux measurements with pure water as feed solution, is used to describe the membrane productivity throughout the text. [3, 56, 57] The SA concentrations were obtained using a Shimadzu total organic carbon (TOC) analyzer (Shimadzu Co., Japan) and the rejection rate was calculated by eq (2).[10]

$$R_{SA}(\%)=(1-\frac{C_p}{C_f})\times 100 \quad (2)$$

Long-term fouling tests were performed to obtain information on the antifouling properties of the membranes. [58] The flux recovery ratio (FRR), the total flux decline ratio (DR_t), the reversible flux decline ratio (DR_r), and the irreversible flux decline ratio (DR_{ir}) were used as parameters to describe the fouling behavior: [59]

$$FRR=\frac{J_2}{J_1}\times 100\% \quad (3)$$

$$DR_t=\left(1-\frac{J_p}{J_1}\right)\times 100\% \quad (4)$$

$$DR_r=\frac{J_2-J_p}{J_1}\times 100\% \quad (5)$$

$$DR_{ir}=\left(1-\frac{J_2}{J_1}\right)\times 100\% \quad (6)$$

where J_1 (L $m^{-2}h^{-1}$) is the pure water flux, J_p (L $m^{-2}h^{-1}$) is the SA solution flux, and J_2 (L $m^{-2}h^{-1}$) is the pure water flux of the clean membrane.

RESULTS AND DISCUSSION

Ternary Phase Diagram. The ternary phase diagram of PVC/solvent (PolarClean or DMAc)/DI water system with and without the additive PVC-g-PEGMA at 60 ℃ is depicted in Figure 1. The data points represent the coagulation value, i.e., the amount of non-solvent that causes a phase inversion at a certain polymer concentration, which in turn reflects the thermodynamic stability of the casting solution. [49, 60] M1-M7 had low coagulation values, which are related to early-stage phase inversion and typically correlated with the formation of porous membranes. While the PVC concentrations were the same for M2-8P and M4-8DMAc solutions, M2 was found to be closer to the polymer-solvent axis, indicating that a lower amount of water is needed to induce phase inversion, that is, lower thermodynamic stability for the system involving PolarClean compared to DMAc. The solubility parameter, Ra, of the couple PVC-PolarClean is slightly higher than that of PVC-DMAc (Table 2), so the compatibility of PVC-PolarClean is a bit poorer, meaning that PolarClean had weaker solvent power with respect to PVC. Weaker solvent power translates into a lower amount of water needed to induce polymer precipitation, [61] which is in good agreement with the coagulation value.

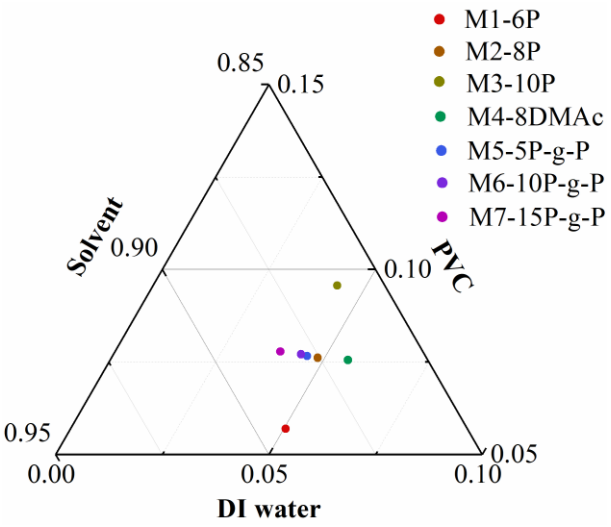

Figure 1. Ternary phase diagram of PVC/solvent (PolarClean or DMAc)/DI water system with and without the amphiphilic additive PVC-g-PEGMA at 60 ℃.

Table 2. Hansen Solubility Parameter and Ra Values of PVC and Different Solvents.

Materials	Hansen solubility parameters			Ra
	δ_d	δ_p	δ_h	
PVC [62]	18.7	10.0	3.1	-
DMAc [62]	16.8	11.5	10.2	8.19
PolarClean [46, 47]	15.8	10.7	9.2	8.45

When the amphiphilic additive was added to the membrane casting solution, the cloud point significantly shifted towards the polymer-solvent axis, and shifted more with the increase of the additive amount. This result indicates that the presence of PVC-g-PEGMA can accelerate the precipitation rate. Faster precipitation rate commonly promotes the formation of macrovoids in the sublayer and of larger pores at the surface. [63] This mechanism was corroborated by higher overall porosities and larger pore size than in the case of pure PVC membranes, as summarized below in Table 3.

Membrane Morphology. The results of surface and cross-section morphologies are summarized in Figure 2 and Figure 3. For each composition, several randomly selected images were binarized using Image Pro Plus V.7.0 software (Media Cybernetics, USA). The following statistical information was obtained from the SEM images and is summarized in Table 3, together with the total membrane porosity values: average pore diameter ($D_{average}$), maximum pore diameter (D_{max}), pore density, and surface porosity. The surface porosity is defined as the total surface area enclosed by pore inlets divided by the unit area of the entire separation surface. [64] It is different from the total porosity, which is the proportion of pore volume to total volume of

membrane in its entire thickness, and is determined according to Eq (1). Figure 2 presents the effect of PVC concentrations on membrane morphology. With the increase of PVC concentration, the membrane structure became denser, with a lower density of pores of smaller size at the surface, as well as a smaller total porosity. This result can be explained by the higher viscosity of the dope solutions containing higher PVC concentrations, which hindered the exchange of solvent and non-solvent and slowed down the rate of phase inversion. [3, 50] Concurrently, the root mean square (RMS) roughness values decreased significantly with the increase of PVC concentration, as lower porosity and smaller surface pores are usually correlated with smoother surfaces. [65, 66]

It is interesting again to compare M4-DMAc with M2-8P, both cast from solutions with the same PVC concentration 8%, but with completely different final morphologies. The only possible conclusion is that the effect of solvent on membrane morphology was significant. When the traditional solvent DMAc was used, the resulting membrane had larger pore sizes and a wider range of pore distribution on the surface compared to the membrane fabricated using PolarClean. While the use of PolarClean promotes an earlier phase separation, PolarClean has lower diffusivity in water than DMAc, which led to smaller and more uniform pores when solvent and non-solvent exchange occurred.

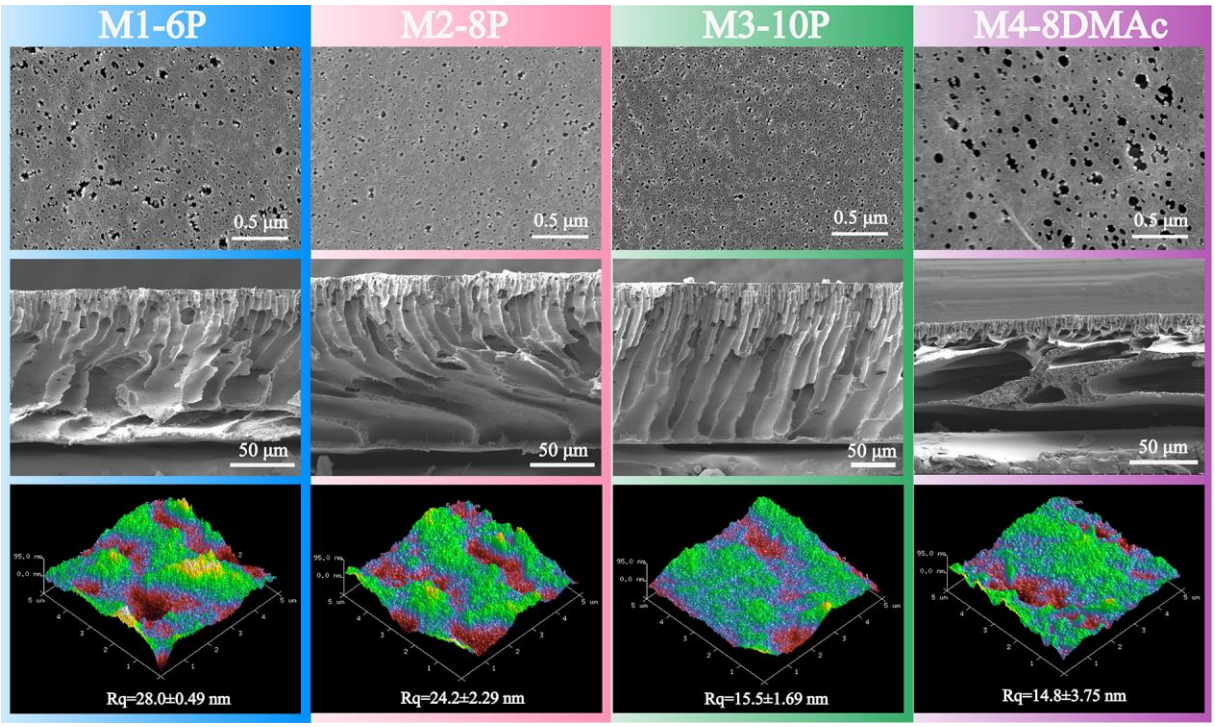

Figure 2. Representative SEM micrographs of the membrane surfaces and cross-sections and AFM images of the membrane surfaces. The membranes were made from PVC dissolved in the solvent PolarClean at different polymer concentrations (M1-6P, M2-8P, M3-10P) and from PVC dissolved in DMAc at one concentration (M4-8DMAc). All surface images were obtained under magnification 50 K×, while the cross-sectional images were obtained under magnification 500×, except for M3-10P, for which the magnification was 300×.

Figure 3 shows the effect of additive amount and of PET support layer on membrane morphology when both the solvent and the concentration of PVC were kept constant, namely, PolarClean and 8%, respectively. Compared with PVC-only membrane M2, adding PVC-g-PEGMA enlarged the cross-sectional membrane pore size, thus the total porosity, but it significantly reduced surface porosity. These effects were more pronounced as the proportion of additive increased. The total porosity in the presence of the amphiphilic additive was larger due

to accelerated phase separation, resulting in wider finger-like cross-sectional voids. The smoother surfaces compared to M2 may also be explained with the lower pore density and surface porosity of the membranes obtained from blended dope solutions. [66]

The use of PET fabrics as support layer also significantly affected the membrane morphology, specifically increasing all the surface porosity parameters; see M5-5P-g-P and M8-5P-g-P^{SL}. The average pore size, max pore size, pore density, and surface porosity for M5 (no support layer) were 23 nm, 28 nm, 1.2×10^{13} m^{-2}, and 0.48 %, respectively, while those for M8 were 26 nm, 31 nm, 3.5×10^{13} m^{-2}, and 2.02 %. This effect of increased surface porosity is consistent with other studies. [67, 68] The PET support layer can promote the formation of surface pores as it hinders the lateral shrinkage when the membrane is immersed into the coagulation bath. [67] These mechanisms end up causing a lower total porosity (85.5~~48~~±3.8~~0~~ % for M8) but a more porous and smoother membrane surface. [67]

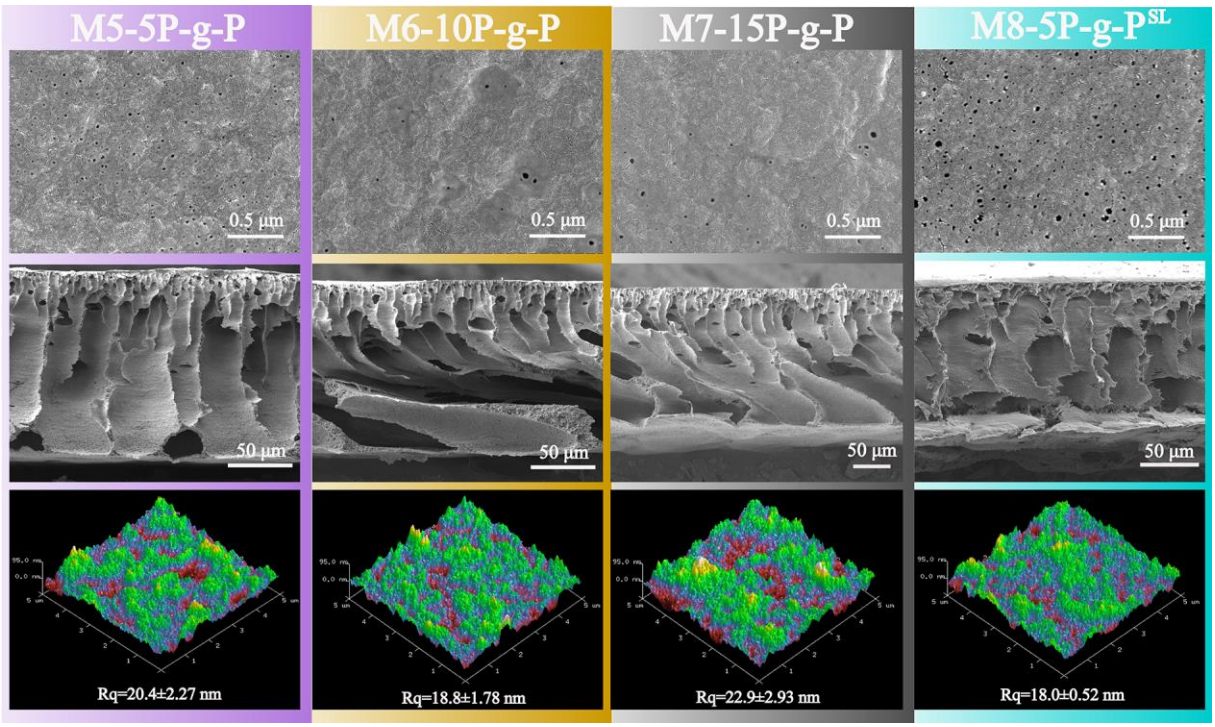

Figure 3. Representative SEM micrographs of the membrane surfaces and cross-sections and AFM images membrane surfaces. The membranes were fabricated using blends of PVC and PVC-g-PEGMA dissolved in the solvent PolarClean without PET support layer (M5-5P-g-P, M6-10P-g-P, M7-15P-g-P) and with PET support layer (M8-5P-g-P^{SL}). All surface images were obtained under magnification 50 K×, while the cross-sectional images were obtained under magnification 500× for M5 and M6, 300× for M7, and 400× for M8.

Table 3. Statistics of Average Pore Diameter ($D_{average}$), Maximum Pore Diameter (D_{max}), Pore Density, Surface Porosity, and Total Porosity for All Membranes.

Membrane ID	$D_{average}$ (nm)	D_{max} (nm)	Pore density (m^{-2})	Surface porosity (%)	Total porosity (%)
M1-6P	27	35	4.8×10^{13}	2.98	88.658 ± 4.798

M2-8P	24	30	2.8×10^{13}	1.32	88.78±2.72
M3-10P	21	27	3.1×10^{13}	1.01	86.44±3.34
M4-8DMAc	41	55	6.2×10^{13}	11.5	80.50±7.106
M5-5P-g-P	23	28	1.2×10^{13}	0.48	94.43±3.44
M6-10P-g-P	30	34	3.6×10^{12}	0.27	89.988±4.42
M7-15P-g-P	33	38	2.8×10^{12}	0.26	95.00±3.31
M8-5P-g-P^{SL}	26	31	3.5×10^{13}	2.02	85.548±3.80

Near-Surface Element Composition. The XPS spectra and fitted C 1s regions for M1-M8 are presented in Figure 4, as obtained by CasaXPS processing software (Casa Software Ltd., England). All membranes showed peaks for carbon (C), oxygen (O), and chlorine (Cl). For pure PVC membranes M1-M4, the signal of O should not exist since no oxygen-containing additive was used in the dope solution. The reason for the small peaks of O 1s may be the adsorption of H_2O from air humidity [69] or a small amount of solvent remaining on the membrane surface (the solvents PolarClean and DMAc all have C=O bonds). [70]

For M5-M7, the existence of O-C=O (288.2 eV) and C-O (286.4 eV) groups proved the successful synthesis and inclusion of PVC-g-PEGMA. During phase inversion, the hydrophilic PEGMA segments were enriched at the membrane surface and the hydrophobic segments tended to be entangled with the membrane matrix. [71] The mole fraction of PEGMA at the near-surface was calculated by eq (7): [72, 73]

$$X^{PEGMA} = \frac{A_{COO}}{A_{COO} + A_{CHCl}} \tag{7}$$

where A_{COO} and A_{CHCl} are the areas of the fitted COO and CHCl peaks. The near-surface weight fraction of PEGMA (ϕ^{PEGMA}) was calculated by the molecular weights of PEGMA and that of a unit PVC. The weight fractions of PEGMA for M5-5P-g-P, M6-10P-g-P and M7-15P-g-P were

40%, 38% and 36%, respectively, which implies that the number of PEGMA segments in the near-surface decreased with the increase of PVC-g-PEGMA amount in the dope solution. Based on the results of ternary phase diagram, one of the reasons was the quicker precipitation at higher amount of additive, with PEGMA not having sufficient time to migrate to the near-surface. [73] M6-10P-g-P had the highest oxygen content of 11.8%, then followed by M7-15P-g-P (9.3%) and M5-10P-g-P (9.1%). The higher oxygen content tends to result in more hydrophilic membrane surface and better anti-fouling property. [74] The oxygen content is not a simple correspondence with the weight fraction of the -COO functional group, and the spatial arrangement of the functional groups also plays an important role.

Comparing M5-5P-g-P with M8-5P-g-P^{SL}, the weight fraction of PEGMA decreased when non-woven PET fabrics support layer was used (40% for M5 and 34% for M8), indicating that the support layer thwarted the transfer and enrichment of PEGMA segments to some extent. ATR-FTIR spectra are consistent with this discussion; the spectra results and analyses are summarized in Figure S2 and Text S6 (SI).

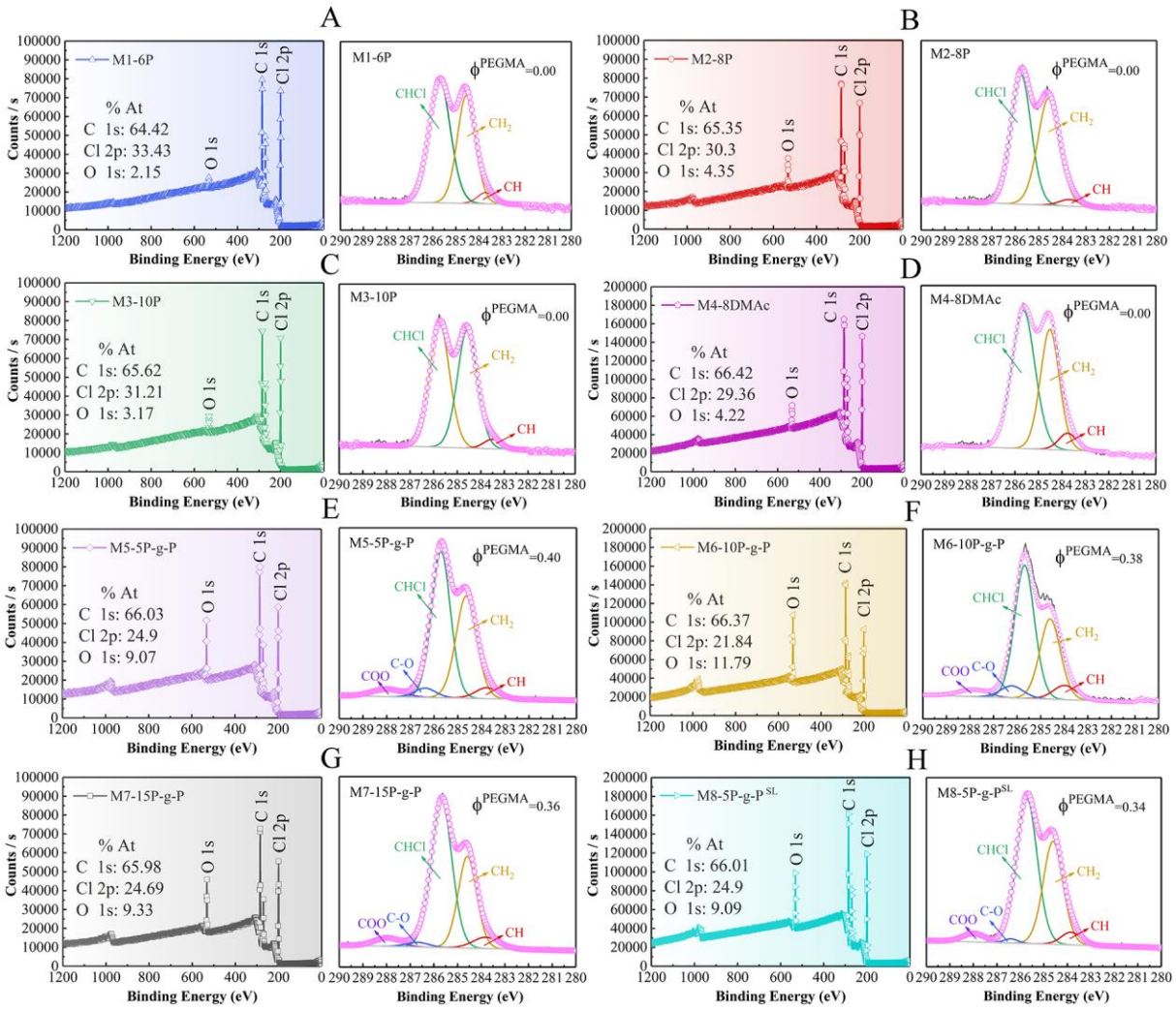

Figure 4. XPS spectra and fitted C 1s regions for pure PVC membrane M1-M4 and for PVC/PVC-g-PEGMA blended membrane M5-M8: (A) M1-6P, (B) M2-8P, (C) M3-10P, (D) M4-8DMAc, (E) M5-5P-g-P, (F) M6-10P-g-P, (G) M7-15P-g-P and (H) M8-5P-g-P^{SL}. The elements atom percent and weight fraction of PEGMA are indicated in each graph.

Wettability of the Membranes. Changes of the contact angles versus time for pure PVC membranes and PVC/PVC-g-PEGMA blended membranes are shown in Figure 5. For M1-M3, with the increase of PVC concentrations from 6% to 10%, the contact angles decreased. This trend is especially pronounced for M3-10P, for which the contact angle was significantly lower

compared to M1 and M2. As the membrane chemistry was analogous, this result may be rationalized with smoother surfaces at higher PVC concentrations (see in Figure 2). [22] For membranes fabricated by different solvents with the same PVC concentration of 8%, M4-8DMAc had similar contact angle of M2-8P, even though the roughness value of M4 was only half of M2. These data may suggest that the solvents used for membrane fabrication can also affect the wettability of the resulting membrane.

When PVC-g-PEGMA was added in the dope solution, the hydrophilic PEGMA segments migrated to the surface, resulting in more wettable surfaces compared with pure PVC membranes. [73] More PEGMA segments and smoother surface will result in more wettable surfaces. Indeed, these two factors contributed to obtain a trend of contact angles with the order M5 > M7 >M6. Regarding the presence of an underlying PET layer, M8-5P-g-P^{SL} had a higher CA than M5-5P-g-P, which can also be explained by the competition between surface PEGMA amount and surface roughness.

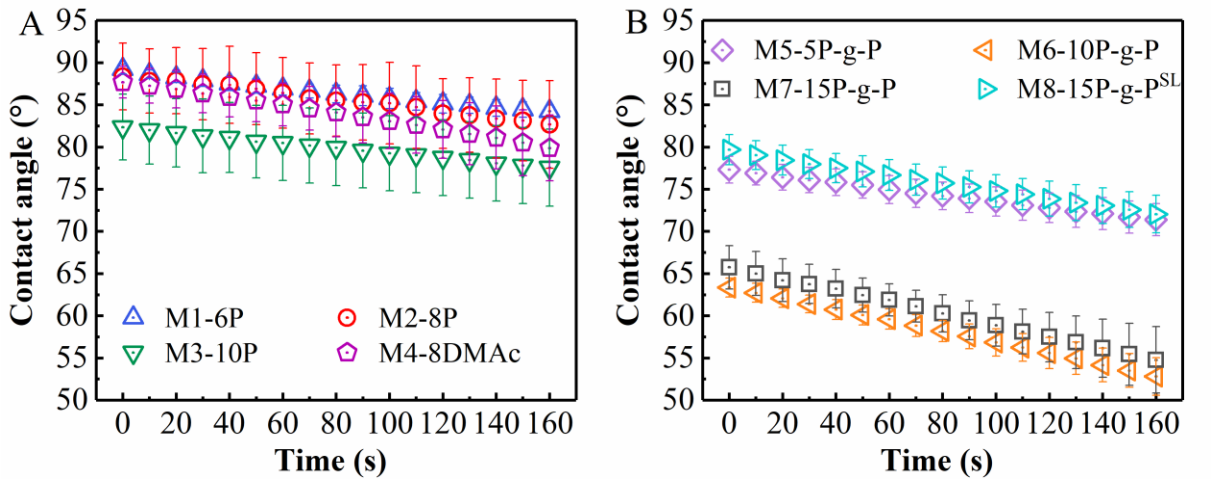

Figure 5. Water contact angles as a function of time for: (A) PVC membranes synthesized with 6-10% PVC concentrations using the solvent PolarClean or DMAc, (B) PVC/PVC-g-PEGMA blended membranes from solutions of 8% PVC in the solvent PolarClean.

Transport Performance. The permeabilities, SA rejection rates, and flux recovery ratios of pure PVC membranes fabricated using the solvents PolarClean or DMAc are shown in Figure 6A and Figure 6B. The pure water membrane permeability coefficient dropped from 6241 L $m^{-2}h^{-1}bar^{-1}$ (M1-6P) to 3419 L $m^{-2}h^{-1}bar^{-1}$ (M2-8P) and then to 1560 L $m^{-2}h^{-1}bar^{-1}$ (M3-10P) ~~when pure water was used~~, due to the decrease of average pore diameter, pore density, and surface porosity (Table 3). [75] The permeability coefficient of M1 is the highest ~~one we have seen~~that has been reported so far for a PVC membrane. The decrease of pore diameter led to the increase of SA particles rejection from 97.0 ± 0.2% (M1-6P) to 98.3 ± 0.3% (M2-8P) and to 99.2 ± 0.1% (M3-10P). The rejection rates for membranes fabricated by PolarClean were all higher than that of membranes fabricated by traditional solvent DMAc (92.3 ± 0.3%), because the pores were much smaller, as discussed above. [76] When the SA solution was used as feed, the fluxes for all membranes dropped rapidly due to SA particle blocking, and then the fluxes reached similar steady-state levels. After 7 hours of fouling test, a 3 min DI water wash was applied, and the permeability of pure water was measured again ~~using pure water~~ to assess the antifouling property of the membrane. The flux recovery ratios (FRR) for M1-M4 were all below 45%.

Figure 6C displays the permeabilities of PVC/PVC-g-PEGMA blended membranes fabricated using the solvent PolarClean. Compared with M2-8P, adding PVC-g-PEGMA reduced the ~~membrane~~ pure water permeability of the membrane to some extent due to the much lower pore densities and surface porosities of blended membranes. (Table 3). However, when the non-woven PET fabric was used as the support layer, the pure water flux increased and became higher even than that of M2-8P, reaching a value of 5355 L $m^{-2}h^{-1}bar^{-1}$. The SA rejection rates for M5-M8 were all above 97%, suggesting that adding PVC-g-PEGMA and using a support fabric layer had little effect on the rejection performance. Additionally, the antifouling properties

for blended membranes were enhanced compared with pure PVC membranes due to the more wettable surfaces. The FRR values for M5-M8 were 68.8 ± 2.5%, 81.2 ± 0.5%, 77.4 ± 3.5% and 57.0 ± 1.1%, respectively. Other ratios (DR_t, DR_r and DR_{ir}) to assess the antifouling properties are summarized in Figure S4 (SI).

To summarize, all M1-M8 membranes were characterized by~~had~~ high pure water permeability coefficients~~ies~~, larger than 1000 L $m^{-2}h^{-1}bar^{-1}$ ~~when pure water was used~~. Such high permeability values may be attributed to: (i) the thickness of the surface active layer, shown in Figure S5 (SI), (ii) the pore density and the surface porosity, and (iii) the nature of the pore interconnection in the bulk of the membranes. Higher surface porosity and a thinner active layer will lead to lower resistance to filtration, hence higher water permeability. [77-79] Large total porosity (>80 %) also has some contribution to water permeability. [78, 80, 81] M1 and M8 had ultrahigh pure water permeabilities >5000 L m^{-2} h^{-1} bar^{-1}, much larger than other membranes. This result is rationalized with the fact that M1 and M8 had the highest values of pore density (4.8×10^{13} m^{-2} and 3.5×10^{13} m^{-2}) and surface porosity (2.98 % and 2.02 %) among all membranes, which promotes the achievement of high water permeability, as also reported by previous studies. [71, 73, 82, 83] By adding amphiphilic additives PVC-g-PEGMA, the antifouling properties were enhanced to a great extent and membranes retained high SA rejection rate, but the presence of the amphiphilic polymer resulted in lower pure water permeability. To overcome this problem, a non-woven PET may be used as support layer to increase the surface porosity and thus the permeability. LCA analyses have shown that ultrahigh permeability and improved antifouling properties may reduce the environmental impacts related to the membrane use phase. [84-87]

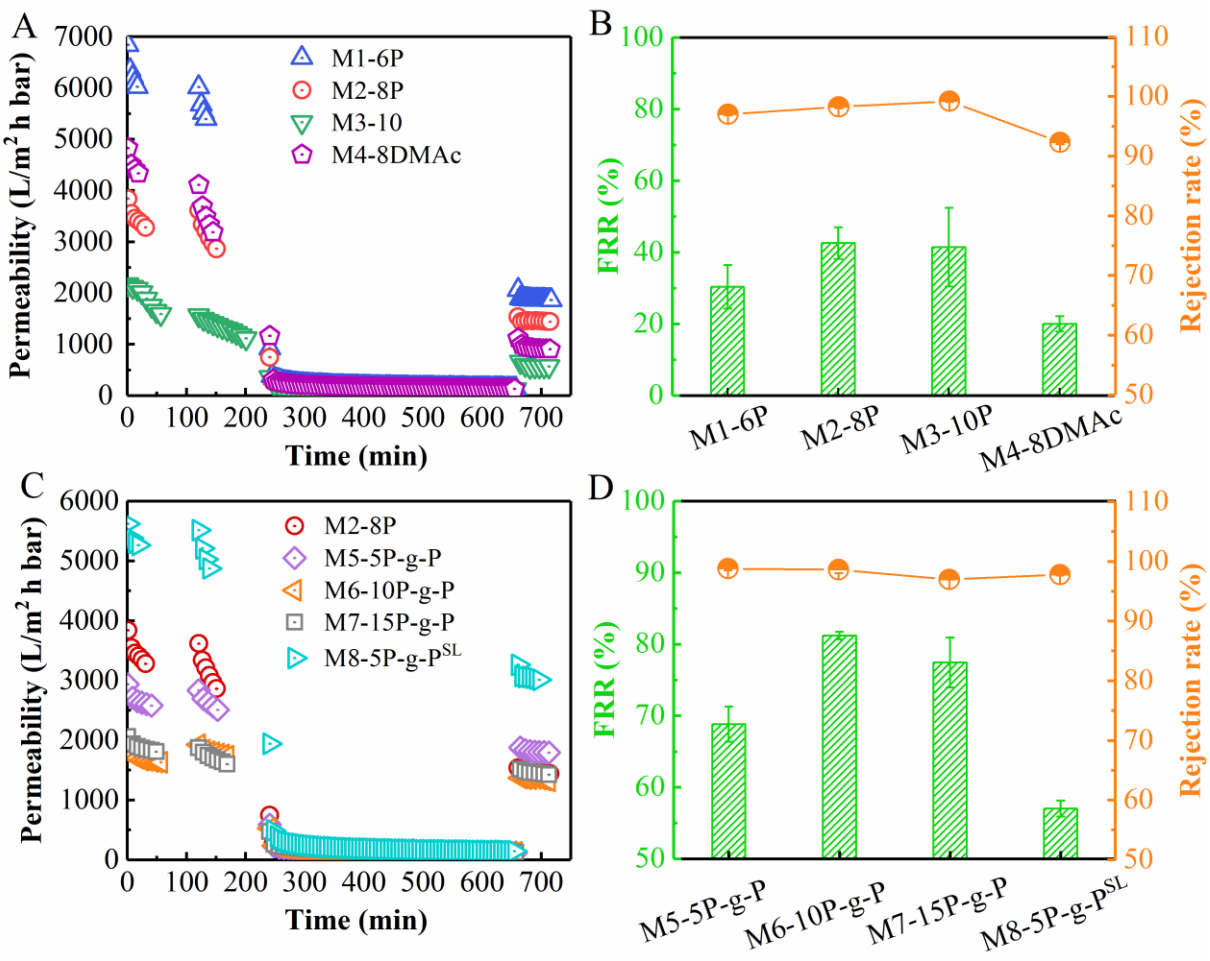

Figure 6. (A) Variations of permeability with time for pure PVC membranes fabricated using PolarClean with 6%, 8% and 10% PVC concentrations and owing DMAc with 8% PVC. (B) Flux recovery ratios (FRR) and SA rejection rates for pure PVC membranes. (C) Variations of permeability with time for PVC/PVC-g-PEGMA blended membranes with 8% PVC concentration fabricated using the solvent PolarClean. (D) Flux recovery ratios (FRR) and SA rejection rates for PVC/PVC-g-PEGMA blended membranes.

CONCLUSION

In this work, PVC ultrafiltration membranes were prepared via NIPS by using the green solvent PolarClean for the first time. At the tested conditions, the membranes prepared using

PolarClean had smaller, more even pores, and narrower pore size distribution compared with the membranes prepared by traditional toxic solvent DMAc, even at low PVC concentration, leading to high SA rejection (> 97.0 ± 0.2%). Meanwhile, with the increase of PVC concentration from 6% to 8% to 10%, the pore size, pore density, surface porosity, and roughness decreased with increased wettability, making the flux decline and SA rejection and antifouling properties improve.

The optimized PVC concentration was 8%. To further improve the membranes, the amphiphilic copolymer PVC-g-PEGMA was added. The blended membrane had much higher FRR with equivalently high SA rejection, however, at the cost of a loss of pure water flux due to the smaller surface porosity. Using a non-woven PET fabric as support layer was a successful strategy to maintain a high surface porosity for the blended membranes. The membrane cast from 8% PVC, 5% amphiphilic additive, and in the presence of a fabric layer ~~had~~ was characterized by an ultrahigh pure water permeability coefficient of > 5000 L $m^{-2}h^{-1}bar^{-1}$ ~~when pure water was used~~, high SA rejection of 97.8 ± 0.2%, and improved flux recovery ratio of 57.0 ± 1.1%. A final comparison of all PVC membranes investigated in this study is presented in Figure 7.

The use of PolarClean as a green solvent in PVC membrane fabrication allows a more sustainable and environmentally friendly manufacturing process, while achieving outstanding overall membrane performance. In other words, the application of this novel green solvent may reduce the environmental impact related to both the manufacturing phase and the use phase of the membrane. In summary, this work indicates that it is possible to use green solvents to replace traditional toxic ones, achieving the simultaneous goals of sustainable production and high membrane performance.

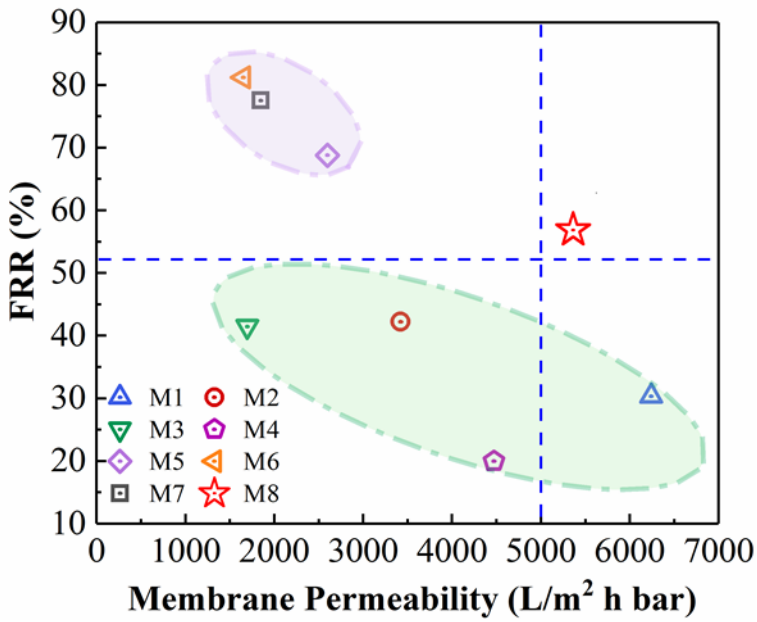

Figure 7. Comparison of the membrane performance of all PVC-based membranes: M1-6P, M2-8P, M3-10P, M4-8DMAc, M5-5P-g-P, M6-10P-g-P, M7-15P-g-P and M8-5P-g-P^{SL}.

ASSOCIATED CONTENT

Supporting Information.

The supporting information is available free of charge.

Six texts, six figures about the detailed experimental procedures and additional experimental data. Figure S1. ^{1}H NMR spectrum of the copolymer PVC-g-PEGMA. Figure S2. ATR-FTIR spectra of pure PVC membranes: M1-6P, M2-8P, M3-10P and M4-8DMAc, and of PVC/PVC-g-PEGMA blended membranes: M5-5P-g-P, M6-10P-g-P, M7-15P-g-P and M8-5P-g-P^{SL}. Figure S3. Molecular structure of PolarClean. Figure S4. FRR (flux recovery ratio), DR_r (reversible flux decline ratio), DR_{ir} (irreversible flux decline ratio) and DR_t (total flux decline ratio) for pure PVC membranes: M1-6P, M2-8P, M3-10P and M4-8DMAc, and for PVC/PVC-g-PEGMA blended membranes:M5-5P-g-P, M6-10P-g-P, M7-15P-g-P and M8-5P-g-P^{SL}. Figure S5.

Representative SEM micrographs of the membrane cross-sections for pure PVC membrane M1-M4 and for PVC/PVC-g-PEGMA blended membrane M5-M8: (A) M1-6P, (B) M2-8P, (C) M3-10P, (D) M4-8DMAc, (E) M5-5P-g-P, (F) M6-10P-g-P, (G) M7-15P-g-P, and (H) M8-5P-g-P^{SL}. All surface images were obtained under magnification 20 K×. Figure S6. ~~The p~~Pure water flux of M1-M8 under different pressures at the temperature of 25 ℃. The membrane effective filtration area was 0.00287 m^2.

AUTHOR INFORMATION

Corresponding Author

Tel.: +86-28-85995998; Fax: +86-28-62138325; E-mail: bcliu@scu.edu.cn; baicangliu@gmail.com (B. Liu).

ORCID

Baicang Liu: 0000-0003-3219-1924

Alberto Tiraferri: 0000-0001-9859-1328

Sheng Chen: 0000-0002-9428-3675

Liang-Yin Chu: 0000-0002-2676-6325

Notes

The authors declare no competing financial interests.

ACKNOWLEDGMENTS

This work was supported by the National Natural Science Foundation of China (51678377), the State Key Laboratory of Separation Membranes and Membrane Processes (Tianjin Polytechnic University) (M2-201809), and the Fundamental Research Funds for the Central Universities. Alberto Tiraferri acknowledges the support of Politecnico di Torino. The views and ideas expressed herein are solely those of the authors and do not represent the ideas of the funding agencies in any form.

REFERENCES

(1) Huang, H.; Yu, J.; Guo, H.; Shen, Y.; Yang, F.; Wang, H.; Liu, R.; Liu, Y., Improved antifouling performance of ultrafiltration membrane via preparing novel zwitterionic polyimide. *Appl. Surf. Sci.* **2018,** *427*, 38-47.

(2) Figoli, A.; Marino, T.; Simone, S.; Di Nicolo, E.; Li, X. M.; He, T.; Tornaghi, S.; Drioli, E., Towards non-toxic solvents for membrane preparation: a review. *Green Chem.* **2014,** *16*, (9), 4034-4059.

(3) Xu, J. A.; Xu, Z. L., Poly(vinyl chloride) (PVC) hollow fiber ultrafiltration membranes prepared from PVC/additives/solvent. *J. Membr. Sci.* **2002,** *208*, (1-2), 203-212.

(4) Zhang, Y.; Tong, X.; Zhang, B.; Zhang, C.; Zhang, H.; Chen, Y., Enhanced permeation and antifouling performance of polyvinyl chloride (PVC) blend Pluronic F127 ultrafiltration membrane by using salt coagulation bath (SCB). *J. Membr. Sci.* **2018,** *548*, 32-41.

(5) Ahmad, T.; Guria, C.; Mandal, A., Optimal synthesis and operation of low-cost polyvinyl chloride/bentonite ultrafiltration membranes for the purification of oilfield produced water. *J. Membr. Sci.* **2018,** *564*, 859-877.

(6) Fan, X.; Su, Y.; Zhao, X.; Li, Y.; Zhang, R.; Zhao, J.; Jiang, Z.; Zhu, J.; Ma, Y.; Liu, Y., Fabrication of polyvinyl chloride ultrafiltration membranes with stable antifouling property by exploring the pore formation and surface modification capabilities of polyvinyl formal. *J. Membr. Sci.* **2014,** *464*, 100-109.

(7) Rana, D.; Matsuura, T., Surface Modifications for Antifouling Membranes. *Chem. Rev.* **2010,** *110*, (4), 2448-2471.

(8) Liu, B.; Chen, C.; Zhang, W.; Crittenden, J.; Chen, Y., Low-cost antifouling PVC ultrafiltration membrane fabrication with Pluronic F 127: Effect of additives on properties and performance. *Desalination* **2012,** *307*, 26-33.

(9) Liu, F.; Hashim, N. A.; Liu, Y.; Abed, M. R. M.; Li, K., Progress in the production and modification of PVDF membranes. *J. Membr. Sci.* **2011,** *375*, (1-2), 1-27.

(10) Wu, H.; Li, T.; Liu, B.; Chen, C.; Wang, S.; Crittenden, J. C., Blended PVC/PVC-g-PEGMA ultrafiltration membranes with enhanced performance and antifouling properties. *Appl. Surf. Sci.* **2018,** *455*, 987-996.

(11) Liu, J.; Su, Y.; Peng, J.; Zhao, X.; Zhang, Y.; Dong, Y.; Jiang, Z., Preparation and Performance of Antifouling PVC/CPVC Blend Ultrafiltration Membranes. *Ind. Eng. Chem. Res.* **2012,** *51*, (24), 8308-8314.

(12) Madaeni, S. S.; Rahimpour, A., Effect of type of solvent and non-solvents on morphology and performance of polysulfone and polyethersulfone ultrafiltration membranes for milk concentration. *Polym. Adv. Technol.* **2005,** *16*, (10), 717-724.

(13) Anastas, P.; Eghbali, N., Green chemistry: principles and practice. *Chem. Soc. Rev.* **2010,** *39*, (1), 301-312.

(14) Capello, C.; Fischer, U.; Hungerbuehler, K., What is a green solvent? A comprehensive framework for the environmental assessment of solvents. *Green Chem.* **2007,** *9*, (9), 927-934.

(15) Byrne, F. P.; Jin, S.; Paggiola, G.; Petchey, T. H. M.; Clark, J. H.; Farmer, T. J.; Hunt, A. J.; Robert McElroy, C.; Sherwood, J., Tools and techniques for solvent selection: green solvent selection guides. *Sustainable Chem. Processes* **2016,** *4*, (1), 1-24.

(16) Clarke, C. J.; Tu, W.-C.; Levers, O.; Brohl, A.; Hallett, J. P., Green and Sustainable Solvents in Chemical Processes. *Chem. Rev.* **2018,** *118*, (2), 747-800.

(17) Fadhil, S.; Marino, T.; Makki, H. F.; Alsalhy, Q. F.; Blefari, S.; Macedonio, F.; Di Nicolo, E.; Giorno, L.; Drioli, E.; Figoli, A., Novel PVDF-HFP flat sheet membranes prepared by triethyl phosphate (TEP) solvent for direct contact membrane distillation. *Chem. Eng. Process.* **2016,** *102*, 16-26.

(18) Chang, J.; Zuo, J.; Zhang, L.; O'Brien, G. S.; Chung, T.-S., Using green solvent, triethyl phosphate (TEP), to fabricate highly porous PVDF hollow fiber membranes for membrane distillation. *J. Membr. Sci.* **2017,** *539*, 295-304.

(19) Zhao, J.; Chong, J. Y.; Shi, L.; Wang, R., Explorations of combined nonsolvent and thermally induced phase separation (N-TIPS) method for fabricating novel PVDF hollow fiber membranes using mixed diluents. *J. Membr. Sci.* **2019,** *572*, 210-222.

(20) Yeow, M. L.; Liu, Y. T.; Li, K., Morphological study of poly(vinylidene fluoride) asymmetric membranes: Effects of the solvent, additive, and dope temperature. *J. Appl. Polym. Sci.* **2004,** *92*, (3), 1782-1789.

(21) Marti, M.; Molina, L.; Aleman, C.; Armelin, E., Novel Epoxy Coating Based on DMSO as a Green Solvent, Reducing Drastically the Volatile Organic Compound Content and Using Conducting Polymers As a Nontoxic Anticorrosive Pigment. *ACS Sustainable Chem. Eng.* **2013,** *1*, (12), 1609-1618.

(22) Meringolo, C.; Mastropietro, T. F.; Poerio, T.; Fontananova, E.; De Filpo, G.; Curcio, E.; Di Profio, G., Tailoring PVDF Membranes Surface Topography and Hydrophobicity by a

Sustainable Two-Steps Phase Separation Process. *ACS Sustainable Chem. Eng.* **2018,** *6*, (8), 10069-10077.

(23) Meringolo, C.; Mastropietro, T. F.; Poerio, T.; Fontananova, E.; De Filpo, G.; Curcio, E.; Di Profio, G., Tailoring PVDF membranes surface topography and hydrophobicity by a sustainable two-steps phase separation process. *ACS Sustainable Chem. Eng.* **2018,** *6*, (8), 1069-1077.

(24) Wang, S.-Y.; Fang, L.-F.; Cheng, L.; Jeon, S.; Kato, N.; Matsuyama, H., Novel ultrafiltration membranes with excellent antifouling properties and chlorine resistance using a poly(vinyl chloride)-based copolymer. *J. Membr. Sci.* **2018,** *549*, 101-110.

(25) Arthanareeswaran, G.; Starov, V. M., Effect of solvents on performance of polyethersulfone ultrafiltration membranes: Investigation of metal ion separations. *Desalination* **2011,** *267*, (1), 57-63.

(26) Evenepoel, N.; Wen, S.; Tsehaye, M. T.; Van der Bruggen, B., Potential of DMSO as greener solvent for PES ultra- and nanofiltration membrane preparation. *J. Appl. Polym. Sci.* **2018,** *135*, (28), 46494.

(27) Abdullah, A. G.; Fahrina, A.; Maimun, T.; Humaira, S.; Rosnelly, C. M.; Lubis, M. R.; Bahrina, I.; Sunarya, R.; Ghufran, A.; Arahman, N.; Nandiyanto, A. B. D., The morphology and filtration performances of poly(ether sulfone) membrane fabricated from different polymer solution. *MATEC Web of Conferences* **2018,** *197*, 09001.

(28) Paseta, L.; Navarro, M.; Coronas, J.; Téllez, C., Greener processes in the preparation of thin film nanocomposite membranes with diverse metal-organic frameworks for organic solvent nanofiltration. *J. Ind. Eng. Chem.* **2019,** *77*, 344-354.

(29) Fang, C.; Jeon, S.; Rajabzadeh, S.; Cheng, L.; Fang, L.; Matsuyama, H., Tailoring the surface pore size of hollow fiber membranes in the TIPS process. *J. Mater. Chem. A* **2018,** *6*, (2), 535-547.

(30) Fang, C.; Jeon, S.; Rajabzadeh, S.; Fang, L.; Cheng, L.; Matsuyama, H., Tailoring both the surface pore size and sub-layer structures of PVDF membranes prepared by the TIPS process with a triple orifice spinneret. *J. Mater. Chem. A* **2018,** *6*, (42), 20712-20724.

(31) Cui, Z.; Hassankiadeh, N. T.; Lee, S. Y.; Lee, J. M.; Woo, K. T.; Sanguineti, A.; Arcella, V.; Lee, Y. M.; Drioli, E., Poly(vinylidene fluoride) membrane preparation with an environmental diluent via thermally induced phase separation. *J. Membr. Sci.* **2013,** *444*, 223-236.

(32) Cui, Z.; Hassankiadeh, N. T.; Lee, S. Y.; Woo, K. T.; Lee, J. M.; Sanguineti, A.; Arcella, V.; Lee, Y. M.; Drioli, E., Tailoring novel fibrillar morphologies in poly(vinylidene fluoride) membranes using a low toxic triethylene glycol diacetate (TEGDA) diluent. *J. Membr. Sci.* **2015,** *473*, 128-136.

(33) Renner, R., Ionic liquids: An industrial cleanup solution. *Environ. Sci. Technol.* **2001,** *35*, (19), 410-413.

(34) Xing, D. Y.; Chan, S. Y.; Chung, T.-S., Fabrication of porous and interconnected PBI/P84 ultrafiltration membranes using [EMIM]OAc as the green solvent. *Chem. Eng. Sci.* **2013,** *87*, 194-203.

(35) Xing, D. Y.; Dong, W. Y.; Chung, T.-S., Effects of Different Ionic Liquids as Green Solvents on the Formation and Ultrafiltration Performance of CA Hollow Fiber Membranes. *Ind. Eng. Chem. Res.* **2016,** *55*, (27), 7505-7513.

(36) Falca, G.; Musteata, V.-E.; Behzad, A. R.; Chisca, S.; Nunes, S. P., Cellulose hollow fibers for organic resistant nanofiltration. *J. Membr. Sci.* **2019,** *586*, 151-161.

(37) Luciani, L.; Goff, E.; Lanari, D.; Santoro, S.; Vaccaro, L., Waste-minimised copper-catalysed azide–alkyne cycloaddition in Polarclean as a reusable and safe reaction medium. *Green Chem.* **2018,** *20*, (1), 183-187.

(38) Ferlin, F.; Luciani, L.; Viteritti, O.; Brunori, F.; Piermatti, O.; Santoro, S.; Vaccaro, L., Polarclean as a Sustainable Reaction Medium for the Waste Minimized Synthesis of Heterocyclic Compounds. *Front. Chem.* **2019,** *6*.

(39) Dong, X.; Al-Jumaily, A.; Escobar, I. C., Investigation of the Use of a Bio-Derived Solvent for Non-Solvent-Induced Phase Separation (NIPS) Fabrication of Polysulfone Membranes. *Membranes* **2018,** *8*, (2).

(40) Hassankiadeh, N. T.; Cui, Z.; Kim, J. H.; Shin, D. W.; Lee, S. Y.; Sanguineti, A.; Arcella, V.; Lee, Y. M.; Drioli, E., Microporous poly(vinylidene fluoride) hollow fiber membranes fabricated with PolarClean as water-soluble green diluent and additives. *J. Membr. Sci.* **2015,** *479*, 204-212.

(41) Pastore, B. M.; Savelski, M. J.; Slater, C. S.; Richetti, F. A., Life cycle assessment of N-methyl-2-pyrrolidone reduction strategies in the manufacture of resin precursors. *Clean Technol. Environ. Policy* **2016,** *18*, (8), 2635-2647.

(42) Faggian, V.; Scanferla, P.; Paulussen, S.; Zuin, S., Combining the European chemicals regulation and an (eco)toxicological screening for a safer membrane development. *J. Clean. Prod.* **2014,** *83*, 404-412.

(43) Shiu, H.-Y.; Lee, M.; Chao, Y.; Chang, K.-C.; Hou, C.-H.; Chiueh, P.-T., Hotspot analysis and improvement schemes for capacitive deionization (CDI) using life cycle assessment. *Desalination* **2019,** *468*, 114087.

(44) Simon, B.; Bachtin, K.; Kiliç, A.; Amor, B.; Weil, M., Proposal of a framework for scale-up life cycle inventory: A case of nanofibers for lithium iron phosphate cathode applications. *Integr. Environ. Asses.* **2016,** *12*, (3), 465-477.

(45) Cseri, L.; Szekely, G., Towards cleaner PolarClean: Efficient synthesis and extended applications of the polar aprotic solvent methyl 5-(dimethylamino)-2-methyl-5-oxopentanoate. *Green Chem.* **2019,** *21*, (15), 4178-4188.

(46) Jung, J. T.; Kim, J. F.; Wang, H. H.; di Nicolo, E.; Drioli, E.; Lee, Y. M., Understanding the non-solvent induced phase separation (NIPS) effect during the fabrication of microporous PVDF membranes via thermally induced phase separation (TIPS). *J. Membr. Sci.* **2016,** *514*, 250-263.

(47) Jung, J. T.; Wang, H. H.; Kim, J. F.; Lee, J.; Kim, J. S.; Drioli, E.; Lee, Y. M., Tailoring nonsolvent-thermally induced phase separation (N-TIPS) effect using triple spinneret to fabricate high performance PVDF hollow fiber membranes. *J. Membr. Sci.* **2018,** *559*, 117-126.

(48) Marino, T.; Blasi, E.; Tornaghi, S.; Di Nicolò, E.; Figoli, A., Polyethersulfone membranes prepared with Rhodiasolv®Polarclean as water soluble green solvent. *J. Membr. Sci.* **2018,** *549*, 192-204.

(49) Wang, H. H.; Jung, J. T.; Kim, J. F.; Kim, S.; Drioli, E.; Lee, Y. M., A novel green solvent alternative for polymeric membrane preparation via nonsolvent-induced phase separation (NIPS). *J. Membr. Sci.* **2019,** *574*, 44-54.

(50) Russo, F.; Castro-Muñoz, R.; Galiano, F.; Figoli, A., Unprecedented preparation of porous Matrimid® 5218 membranes. *J. Membr. Sci.* **2019,** *585*, 166-174.

(51) Xie, W.; Li, T.; Chen, C.; Wu, H.; Liang, S.; Chang, H.; Liu, B.; Drioli, E.; Wang, Q.; Crittenden, J. C., Using the Green Solvent Dimethyl Sulfoxide To Replace Traditional Solvents Partly and Fabricating PVC/PVC-g-PEGMA Blended Ultrafiltration Membranes with High Permeability and Rejection. *Ind. Eng. Chem. Res.* **2019,** *58*, (16), 6413-6423.

(52) Tiraferri, A.; Yip, N. Y.; Phillip, W. A.; Schiffman, J. D.; Elimelech, M., Relating performance of thin-film composite forward osmosis membranes to support layer formation and structure. *J. Membr. Sci.* **2011,** *367*, (1), 340-352.

(53) Shi, L.; Wang, R.; Cao, Y.; Liang, D. T.; Tay, J. H., Effect of additives on the fabrication of poly(vinylidene fluoride-co-hexafluropropylene) (PVDF-HFP) asymmetric microporous hollow fiber membranes. *J. Membr. Sci.* **2008,** *315*, (1), 195-204.

(54) Tang, C. Y.; Kwon, Y.-N.; Leckie, J. O., Effect of membrane chemistry and coating layer on physiochemical properties of thin film composite polyamide RO and NF membranes: I. FTIR and XPS characterization of polyamide and coating layer chemistry. *Desalination* **2009,** *242*, (1), 149-167.

(55) Fang, L.-F.; Zhu, B.-K.; Zhu, L.-P.; Matsuyama, H.; Zhao, S., Structures and antifouling properties of polyvinyl chloride/poly(methyl methacrylate)-graft-poly(ethylene glycol) blend membranes formed in different coagulation media. *J. Membr. Sci.* **2017,** *524*, 235-244.

(56) Galiano, F.; Figoli, A.; Deowan, S. A.; Johnson, D.; Altinkaya, S. A.; Veltri, L.; De Luca, G.; Mancuso, R.; Hilal, N.; Gabriele, B.; Hoinkis, J., A step forward to a more efficient wastewater treatment by membrane surface modification via polymerizable bicontinuous microemulsion. *J. Membr. Sci.* **2015,** *482*, 103-114.

(57) Li, F.; Meng, J.; Ye, J.; Yang, B.; Tian, Q.; Deng, C., Surface modification of PES ultrafiltration membrane by polydopamine coating and poly(ethylene glycol) grafting: Morphology, stability, and anti-fouling. *Desalination* **2014,** *344*, 422-430.

(58) Asatekin, A.; Kang, S.; Elimelech, M.; Mayes, A. M., Anti-fouling ultrafiltration membranes containing polyacrylonitrile-graft-poly (ethylene oxide) comb copolymer additives. *J. Membr. Sci.* **2007,** *298*, (1-2), 136-146.

(59) Zhao, X.; Su, Y.; Chen, W.; Peng, J.; Jiang, Z., Grafting perfluoroalkyl groups onto polyacrylonitrile membrane surface for improved fouling release property. *J. Membr. Sci.* **2012,** *415*, 824-834.

(60) Wang, D.; Li, K.; Teo, W. K., Relationship between mass ratio of nonsolvent-additive to solvent in membrane casting solution and its coagulation value. *J. Membr. Sci.* **1995,** *98*, (3), 233-240.

(61) García-Fernández, L.; García-Payo, M. C.; Khayet, M., Effects of mixed solvents on the structural morphology and membrane distillation performance of PVDF-HFP hollow fiber membranes. *J. Membr. Sci.* **2014,** *468*, 324-338.

(62) Hansen, C. M., *Hansen Solubility Parameters: a user's handbook*. CRC press: Florida, **2007**.

(63) Young, T.-H.; Chen, L.-W., Pore formation mechanism of membranes from phase inversion process. *Desalination* **1995,** *103*, (3), 233-247.

(64) Hester, J. F.; Banerjee, P.; Mayes, A. M., Preparation of Protein-Resistant Surfaces on Poly(vinylidene fluoride) Membranes via Surface Segregation. *Macromolecules* **1999,** *32*, (5), 1643-1650.

(65) Panda, S. R.; Bhandaru, N.; Mukherjee, R.; De, S., Ultrafiltration of oily waste water: Contribution of surface roughness in membrane properties and fouling characteristics of polyacrylonitrile membranes. *Can. J. Chem. Eng.* **2015,** *93*, (11), 2031-2042.

(66) Jayalakshmi, A.; Rajesh, S.; Mohan, D., Fouling propensity and separation efficiency of epoxidated polyethersulfone incorporated cellulose acetate ultrafiltration membrane in the retention of proteins. *Appl. Surf. Sci.* **2012,** *258*, (24), 9770-9781.

(67) Wang, S.; Li, T.; Chen, C.; Chen, S.; Liu, B.; Crittenden, J., Non-woven PET fabric reinforced and enhanced the performance of ultrafiltration membranes composed of PVDF

blended with PVDF-g-PEGMA for industrial applications. *Appl. Surf. Sci.* **2018,** *435*, 1072-1079.

(68) Lohokare, H. R.; Bhole, Y. S.; Kharul, U. K., Effect of support material on ultrafiltration membrane performance. *J. Appl. Polym. Sci.* **2006,** *99*, (6), 3389-3395.

(69) Xi, Z.-Y.; Xu, Y.-Y.; Zhu, L.-P.; Zhu, B.-K., Modification of polytetrafluoroethylene porous membranes by electron beam initiated surface grafting of binary monomers. *J. Membr. Sci.* **2009,** *339*, (1-2), 33-38.

(70) Alvi, M. A. U. R.; Khalid, M. W.; Ahmad, N. M.; Niazi, M. B. K.; Anwar, M. N.; Batool, M.; Cheema, W.; Rafiq, S., Polymer concentration and solvent variation correlation with the morphology and water filtration analysis of polyether sulfone microfiltration membrane. *Adv. Polym. Tech.* **2019,** *2019*, 1-11.

(71) Shuai, W.; Tong, L.; Chen, C.; Baicang, L.; Crittenden, J. C., PVDF ultrafiltration membranes of controlled performance via blending PVDF-g-PEGMA copolymer synthesized under different reaction times. *Front. Environ. Sci. Eng.* **2018,** *12*, (2), 3.

(72) Hester, J. F.; Banerjee, P.; Won, Y. Y.; Akthakul, A.; Acar, M. H.; Mayes, A. M., ATRP of Amphiphilic Graft Copolymers Based on PVDF and Their Use as Membrane Additives. *Macromolecules* **2002,** *35*, (20), 7652-7661.

(73) Liu, B.; Chen, C.; Li, T.; Crittenden, J.; Chen, Y., High performance ultrafiltration membrane composed of PVDF blended with its derivative copolymer PVDF-g-PEGMA. *J. Membr. Sci.* **2013,** *445*, 66-75.

(74) Yang, B.; Yang, X.; Liu, B.; Chen, Z.; Chen, C.; Liang, S.; Chu, L.-Y.; Crittenden, J., PVDF blended PVDF-g-PMAA pH-responsive membrane: Effect of additives and solvents on membrane properties and performance. *J. Membr. Sci.* **2017,** *541*, 558-566.

(75) Dobosz, K. M.; Kuo-Leblanc, C. A.; Martin, T. J.; Schiffman, J. D., Ultrafiltration Membranes Enhanced with Electrospun Nanofibers Exhibit Improved Flux and Fouling Resistance. *Ind. Eng. Chem. Res.* **2017,** *56*, (19), 5724-5733.

(76) Gao, H.; Sun, X.; Gao, C., Antifouling polysulfone ultrafiltration membranes with sulfobetaine polyimides as novel additive for the enhancement of both water flux and protein rejection. *J. Membr. Sci.* **2017,** *542*, 81-90.

(77) Mulder, M., *Basic Principles of Membrane Technology (second edition)*. 1996.

(78) Benavente, J.; Vázquez, M. I., Effect of age and chemical treatments on characteristic parameters for active and porous sublayers of polymeric composite membranes. *J. Colloid Interface Sci.* **2004,** *273*, (2), 547-555.

(79) Shi, Z.; Zhang, W.; Zhang, F.; Liu, X.; Wang, D.; Jin, J.; Jiang, L., Ultrafast Separation of Emulsified Oil/Water Mixtures by Ultrathin Free-Standing Single-Walled Carbon Nanotube Network Films. *Adv. Mater.* **2013,** *25*, (17), 2422-2427.

(80) Cañas, A.; Ariza, M. J.; Benavente, J., Characterization of active and porous sublayers of a composite reverse osmosis membrane by impedance spectroscopy, streaming and membrane potentials, salt diffusion and X-ray photoelectron spectroscopy measurements. *J. Membr. Sci.* **2001,** *183*, (1), 135-146.

(81) Jonsson, G.; Benavente, J., Determination of some transport coefficients for the skin and porous layer of a composite membrane. *J. Membr. Sci.* **1992,** *69*, (1-2), 29-42.

(82) Tang, Y.; Xu, J.; Gao, C., Ultrafiltration membranes with ultrafast water transport tuned via different substrates. *Chem. Eng. J.* **2016,** *303*, 322-330.

(83) Liu, Q.; Li, L.; Pan, Z.; Dong, Q.; Xu, N.; Wang, T., Inorganic nanoparticles incorporated in polyacrylonitrile-based mixed matrix membranes for hydrophilic, ultrafast, and fouling-resistant ultrafiltration. *J. Appl. Polym. Sci.* **2019,** *136*, (33), 47902.

(84) Ioannou-Ttofa, L.; Foteinis, S.; Chatzisymeon, E.; Fatta-Kassinos, D., The environmental footprint of a membrane bioreactor treatment process through Life Cycle Analysis. *Sci. Total Environ.* **2016,** *568*, 306-318.

(85) Gésan-Guiziou, G.; Sobańtka, A. P.; Omont, S.; Froelich, D.; Rabiller-Baudry, M.; Thueux, F.; Beudon, D.; Tregret, L.; Buson, C.; Auffret, D., Life Cycle Assessment of a milk protein fractionation process: Contribution of the production and the cleaning stages at unit process level. *Sep. Purif. Technol.* **2019,** *224*, 591-610.

(86) Notarnicola, B.; Tassielli, G.; Renzulli, P. A., Environmental and technical improvement of a grape must concentration system via a life cycle approach. *J. Clean. Prod.* **2015,** *89*, 87-98.

(87) Vlasopoulos, N.; Memon, F. A.; Butler, D.; Murphy, R., Life cycle assessment of wastewater treatment technologies treating petroleum process waters. *Sci. Total Environ.* **2006,** *367*, (1), 58-70.

Graphic Abstract

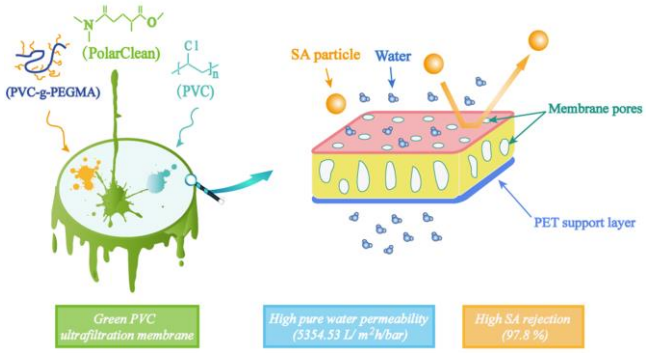

SYNOPSIS

The green and sustainable solvent PolarClean was used to replace traditional solvents and fabricate PVC membrane with improved performance.